

pubs.acs.org/JPCB Article

Bulk Metallic Glasses' Response to Oscillatory Stress Is Governed by the Topography of the Energy Landscape

Longwen Tang, Gang Ma, Han Liu, Wei Zhou,* and Mathieu Bauchy*



Cite This: J. Phys. Chem. B 2020, 124, 11294-11298



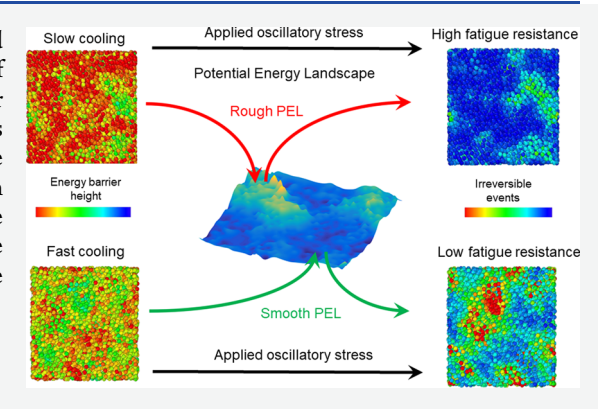
ACCESS

Metrics & More

Article Recommendations

Supporting Information

ABSTRACT: When subjected to cyclic loading, bulk metallic glasses tend to exhibit fatigue-induced damage. Although fatigue is a key limitation of metallic glasses, its atomic origin remains elusive. Here, based on molecular dynamics simulations, we investigate the response of metallic glasses prepared with varying cooling rates to oscillatory stress. We find that fatigue manifests itself as an accumulation of residual strain, which results from some nonaffine displacement of the atoms. Such local reorganizations are promoted under a high cooling rate. Importantly, we demonstrate that the fatigue-induced dynamics of the atoms is encoded in the topography of the static energy landscape, i.e., before any load is applied.



1. INTRODUCTION

Due to their lack of a long-range order, bulk metallic glasses (BMGs) feature unique physical properties, such as a high elastic limit and strong resistance to plastic deformations. However, when subjected to oscillatory loading, BMGs typically suffer from a poor resistance to fatigue. Recent experiments have suggested that the response of BMGs to fatigue strongly depends on the chemical composition, fatigue strongly depends on the chemical composition, leading mode, and cooling rate.

Although this behavior limits the range of application of BMGs, its origin and mechanism remain partially unclear. ^{10,16} The response of BMGs to fatigue can be divided into initiation and propagation stages. ¹⁶ Recent results have suggested that initiation is triggered by the formation of multiple shear bands. ¹⁷ Under monotonic loading, the formation of the shear band arises from the interaction between several critical local rearrangement regions, ^{18,19} which is known as shear transfer zones. ^{20,21} Notably, initiation is greatly facilitated under cyclic stress as compared to monotonic conditions—the mechanism of which remains poorly understood. ²² In particular, the nature of the relationship between the glass structure (and stability thereof) and the propensity for fatigue-induced damage remains elusive. ¹⁰

Herein, to address this question, we investigate the response of an archetypical $\text{Cu}_{64}\text{Zr}_{36}$ BMG to oscillatory stress by molecular dynamics simulations. We find that, at the atomic scale, fatigue manifests itself by some local structural reorganizations. The propensity for such atomic rearrangements depends on the thermal history of the glass and is promoted under high cooling rates. By adopting the activation-relaxation technique (ART), we reveal that the dynamic

response of BMGs to cycling loading is encoded in the topography of their static energy landscape, that is, before any load is applied.

2. METHOD

2.1. Sample Preparation. To establish our conclusions, we simulate an archetypal Cu₆₄Zr₃₆ BMG by molecular dynamics. The system simulated herein comprises 8000 atoms, which are initially randomly placed in a cubic box under periodic boundary conditions. The system is first equilibrated for 1 ns at 2000 K and zero pressure in the isothermal-isobaric (NPT) ensemble with a Nosé-Hoover thermostat, 23,24 such that the simulated melt loses the memory of its initial configuration. The obtained liquid is subsequently cooled to 0 K under zero pressure in the NPT ensemble with varying cooling rates ranging from 10¹⁴ to 10¹⁰ K/s. The interatomic interaction energy is described by the embeddedatom method (EAM) potential, which has been shown to offer a realistic description of the structure and mechanics of Cu-Zr glasses.²⁵ For statistical averaging purposes, a series of 11 glasses are simulated for each cooling rate. The timestep is selected as 1 fs for all simulations. All of the simulations are conducted using the Large-Scale Atomic/Molecular Massively Parallel Simulator (LAMMPS) package. 26

Recived: September 28, 2020 Revised: November 10, 2020 Published: November 24, 2020





2.2. Oscillatory Stress. As illustrated in the inset of Figure 1a, we investigate the fatigue of the simulated Cu₆₄Zr₃₆ BMGs

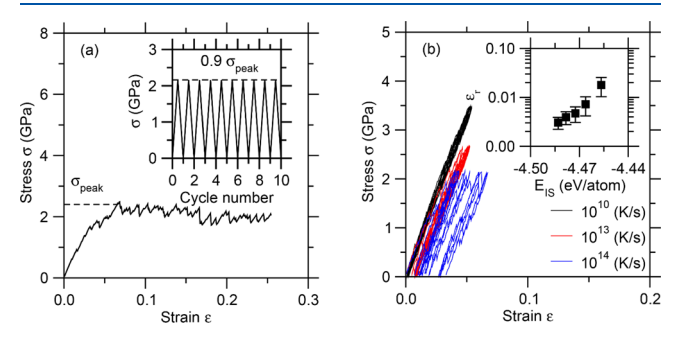


Figure 1. (a) Example of a stress—strain curve for a simulated $\mathrm{Cu}_{64}\mathrm{Zr}_{36}$ bulk metallic glass prepared with a cooling rate of 10^{14} K/s under monotonic tensile deformation, which is used to determine the glass strength (σ_{peak}) . The inset illustrates the series of tensile stress cycles that are then imposed to the simulated glasses. (b) Examples of stress—strain curves upon cycling loading for select cooling rates. The inset shows the residual tensile strain (ε_r) after 10 loading—unloading cycles as a function of the inherent structure energy of the glass (E_{IS}) . Each point represents an average of 33 results obtained for the same cooling rate, while the error bar indicates the standard deviation of these results.

by subjecting them to a series of strain-controlled uniaxial tensile deformation cycles. To achieve this, the system is first deformed along the z-axis by small increments of strain of 0.005%. During the deformation, a zero stress is imposed along the other directions by adjusting the simulation box size at each step of the deformation by energy minimization (using the conjugate gradient algorithm). The stress is then measured after each step of deformation. This process is repeated until the tensile normal stress σ_z reaches $0.9\sigma_{\rm peak}$, where $\sigma_{\rm peak}$ is the glass strength, that is, the maximum normal stress before fracture upon monotonic loading (see Figure 1a). The BMGs are then subjected to unloading using the same methodology until the tensile normal stress is fully released (i.e., $\sigma_z = 0$). The simulated BMGs are subjected to a total of 10 of such loading-unloading cycles (see the inset of Figure 1a). We find that this number of cycles is large enough for the system to reach the steady state—since subsequent cycles do not result in any additional residual strain or any further increase in the potential energy (see the Supporting Information). For each system, such oscillatory stress simulations are then repeated by deforming the BMGs along the x- and y-axis for statistical averaging purposes. It should be noted that the whole deformation process is conducted under athermal and quasistatic conditions, which has been shown to capture the main atomic-scale features of the deformation mechanism of disordered solids. 18,25

2.3. Structural Rearrangements. To characterize the nature of the structural rearrangements occurring within the atomic structure of the simulated glasses upon oscillatory stress, we compute the cumulative nonaffine displacement D of each atom during the whole cycling process. Note that, here, rather than using the conventional nonaffine square displacement D_{\min}^2 proposed in ref 20, we compute the sum of the individual nonaffine displacements experienced by the atoms during each deformation cycle:

$$D = \sum_{i=1}^{n} \sqrt{\Delta D_{i,\min}^2} \tag{1}$$

where $D_{i, \min}^2$ is the incremental nonaffine square displacement after each deformation cycle i and n = 10 is the total number of the cycles. The cutoff value used herein to calculate the local affine displacement field is chosen as the minimum after the first peak in the pair distribution function (i.e., 3.75 Å).

2.4. Energy Landscape. We explore how the response of the simulated BMGs to oscillatory stress is encoded in their potential energy landscape (PEL). To this end, we adopt the activation-relaxation technique nouveau (ARTn) algorithm, which enables a systematic search of saddle points within the energy landscape. 27,28 ARTn has been successfully used to characterize the PEL of disordered phases.²⁹⁻³¹ In detail, starting from a local minimum position in the PEL, a random activation displacement is first imposed on a group of atoms centered around the target particle, wherein the cutoff is herein chosen to be the same as that used to calculate the nonaffine displacement, i.e., the extent of the first coordination shell. The perturbed system is then gradually moved toward the nearest saddle point by following the direction of the negative energy curvature,²⁷ until an energy curvature that is lower than 0.005 ${\rm eV}/\mathring{A}^{-2}$ is achieved. For each target particle, we conduct 20 random independent saddle point searches, which is sufficient to ensure the convergence of the energy barrier distribution for $\text{Cu}_{64}\text{Zr}_{36}\,$ BMGs. 29,30,32

3. RESULTS AND DISCUSSION

3.1. Effect of the Cooling Rate on Fatigue. We first explore how the thermodynamic stability of the simulated BMG (i.e., its fictive temperature) affects its response to fatigue. To this end, we subject the simulated BMG to a series of stress-controlled cyclic deformations (see Section 2.2). Figure 1b shows select examples of stress—strain curves upon cyclic loading for simulated $Cu_{64}Zr_{36}$ BMGs prepared with varying cooling rates.

We observe that, upon cyclic loading, the simulated glasses exhibit some irreversible deformations, which manifest themselves by the formation of a nonzero residual normal strain after unloading (i.e., the glass remains permanently elongated). Notably, we observe that glasses prepared with high cooling rates (e.g., $10^{14}~{\rm K/s}$) exhibit significantly higher permanent deformation than their counterparts prepared with lower cooling rates (e.g., 10^{10} K/s). It should be noted that this behavior is not a spurious effect of the magnitude of the stress cycles, since the maximum stress remains fixed at $0.9\sigma_{\rm peak}$ —so that glasses prepared with high cooling rates are actually subjected to smaller stresses since they exhibit lower tensile strength. To relate this behavior to the thermodynamic stability of the simulated BMGs, we then compute their inherent structure potential energy $E_{\rm IS}$. As shown in the inset of Figure 1, we find that the residual strain after 10 loadingunloading cycles increases monotonically with $E_{\rm IS}$. This confirms that more stable glasses (i.e., prepared with lower cooling rates) are more resistant to fatigue.

3.2. Structural Reorganizations. Next, we investigate the nature of the microscopic carriers of the residual strain that accumulates upon oscillatory loading (see Figure 1b). It should be noted that some of the local rearrangements that are activated during loading can be recovered during unloading—which indicates that a fraction of the rearrangements are

reversible. To exclude the influence of such reversible rearrangements, we calculate the nonaffine displacement of each atom during the whole cycling process. This allows us to solely capture the local irreversible rearrangements occurring in the atomic structure after loading—unloading cycles, while filtering out reversible rearrangements (see Section 2.3 for more details). Figure 2 shows the final residual

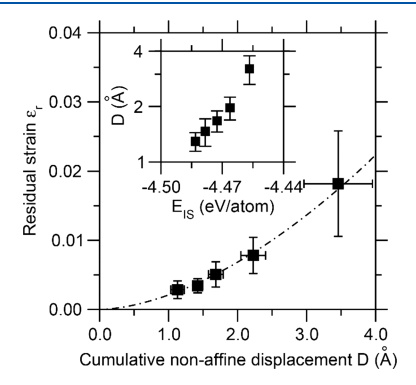


Figure 2. Residual tensile strain as a function of the average cumulative nonaffine displacement D after 10 loading—unloading cycles. The line is to guide the eye. The inset shows the average cumulative nonaffine displacement D as a function of the glass inherent structure energy $E_{\rm IS}$. Each point represents an average of 33 results obtained for the same cooling rate, whereas the error bar indicates the standard deviation of these results.

strain as a function of the cumulative nonaffine displacement for varying cooling rates. We observe that the residual strain increases monotonically with the cumulative nonaffine displacement. This indicates that the fatigue-induced macroscopic irreversible damage manifests itself by some local, nonaffine atomic reorganizations at the atomic scale. As shown in the inset of Figure 2, the average cumulative nonaffine displacement D (i.e., as averaged over all the atoms at fixed cooling rate) increases with $E_{\rm IS}$. This confirms that more stable glasses (i.e., lower $E_{\rm IS}$) are less sensitive to fatigue, at both the macroscopic and atomic scales.

3.3. Fatigue Is Encoded in the Potential Energy Landscape. Having established the relationship between fatigue-induced damage and energetical stability, we now explore whether the sensitivity to fatigue could in some ways be encoded in the underlying PEL. To this end, we compute the distribution of energy barriers accessible to each atom by using the ARTn algorithm (see Section 2.4). Figure 3 shows the distribution of the computed energy barriers for select Cu₆₄Zr₃₆ BMGs with varying cooling rates. We observe that, independently of the cooling rate, the energy barriers exhibit fairly normal distributions. We note that the previously reported excess of small energy barriers³⁰ disappears when the glasses are relaxed at zero temperature and zero stress. Notably, we find that the energy barrier distribution of glasses obtained with low cooling rates tends to shift toward higher energy values as compared to those of glasses formed with higher cooling rates. This indicates that the average height of the energy barriers (E_b , which characterizes the roughness of the PEL) tends to increase upon decreasing the cooling rate. That is, as the cooling rate decreases, the formed glass explores some local states that are deeper within the PEL (i.e., lower $E_{\rm IS}$) and wherein the local minima are separated from each other by larger energy barriers. The monotonic relationship between the depth (i.e., E_{IS}) and the roughness (i.e., E_{b}) of the

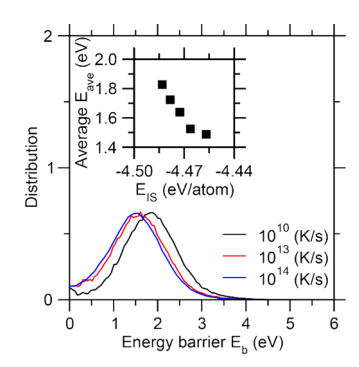


Figure 3. Energy barrier distribution in simulated $\text{Cu}_{64}\text{Zr}_{36}$ bulk metallic glasses prepared with select cooling rates. The inset shows the average value of the energy barrier distributions as a function of the inherent structure energy E_{IS} of the glasses.

local PEL explored by the system upon varying cooling rates is presented in the inset of Figure 3. We note that, upon decreasing the cooling rate, the increase in the height of the energy barriers is notably faster than the decrease in the inherent structure energy of the glass.

We now discuss how the topography of the PEL governs the propensity for BMGs to exhibit microscopic irreversible deformations upon oscillatory stress. Figure 4b shows the cumulative nonaffine displacement D of the atoms within the glass as a function of the average height of the energy barriers that are accessible to them (E_{ave}) . For statistical average purposes, each of the data points shown in Figure 4b corresponds to the values of D and E_{ave} that are averaged over 5% of all of the particles, as sorted in terms of increasing D values. Surprisingly, we observe that the relationship between atomic rearrangements and energy landscape is governed by a clear power-law relationship: $D \propto AE_{\text{ave}}^{-\alpha}$ (a being a power-law exponent), wherein the atomic cumulative nonaffine displacement D decreases upon increasing the average local energy barrier E_{ave} . The power-law relationship may stem from the fractal geometry of the PEL in disordered materials. 34,35 These results demonstrate that the atoms that have locally access to low-energy barriers are more likely to undergo some structural reorganizations upon cyclic loading than those that only have access to large energy barriers. It is remarkable that the fatigue-induced dynamics of the atoms is intrinsically encoded in the static topography of the energy landscape, that is, before any load is applied.

The close relationship between atom dynamics and local energy landscape is further illustrated in Figure 4a, which compares the spatial distribution of D and $E_{\rm ave}$. We observe that the atomic cumulative nonaffine displacement exhibits a notable spatial heterogeneity, at both low and high cooling rates. This is a manifestation of the dynamical heterogeneity that is typically observed in disordered phases. This is a manifestation of D and D are closely mirror each other, wherein regions that are characterized by large atomic displacements are associated with low-energy barriers (i.e., smooth energy landscape) and vice versa. This highlights the fact that, even after having been subjected to several stress cycles, the deformed glasses closely retain the memory of their initial, static energy landscape.

4. CONCLUSIONS

Altogether, our results establish the following atomic picture for the response of $Cu_{64}Zr_{36}$ BMGs to fatigue. Upon loading

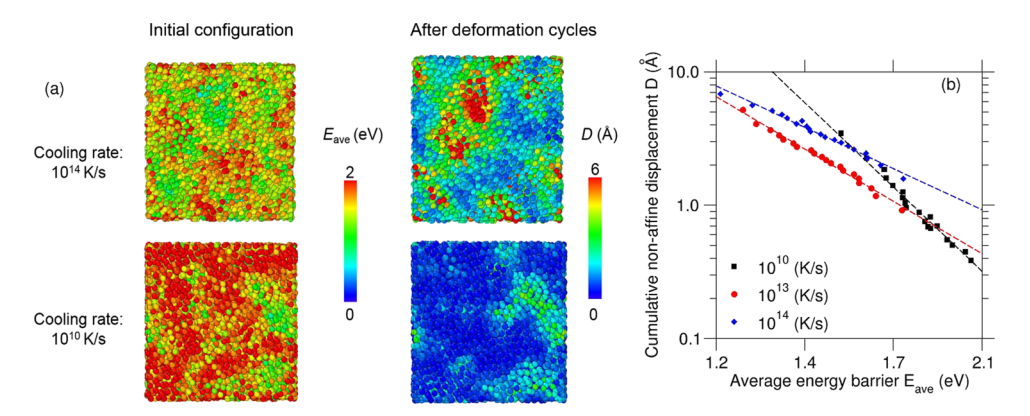


Figure 4. (a) Spatial distributions of the cumulative nonaffine displacement (D) of the atoms and of the average height of the energy barriers that are accessible to them (E_{ave}) for two select cooling rates. (b) Computed values of D as a function of E_{ave} . The lines are some power-law fits.

and unloading, the atoms periodically gain and lose some elastic strain energy, which effectively deforms the local PEL.³ In unstable BMGs formed with high cooling rates, this elastic energy becomes large enough for atoms to overcome local energy barriers and undergo reorganizations. This arises from the fact that such unstable glasses exhibit a smooth energy landscape, with low energy barriers. Some of these nonaffine reorganizations are irreversible, i.e., they are not reversed upon unloading.³⁸ In turn, these atomic-scale reorganizations result in permanent macroscopic deformations (i.e., a residual strain). In contrast, due to the rough nature of their energy landscape (i.e., with large energy barriers), stable BMGs formed with low cooling rates are less prone to nonaffine atomic reorganizations and, hence, less sensitive to fatigue at the macroscopic scale. This mechanism highlights a close correlation between the long-term dynamics of the atoms under cyclic stress and the initial topography of their local energy landscape. This picture echoes recent experiments, indicating that glass annealing can notably enhance BMGs' resistance to fatigue.¹⁴

ASSOCIATED CONTENT

Supporting Information

The Supporting Information is available free of charge at https://pubs.acs.org/doi/10.1021/acs.jpcb.0c08794.

Incremental residual strain as the function of cycle number (Figure S1) and potential energy of the glasses as a function of the number of cycles (Figure S2) (PDF)

AUTHOR INFORMATION

Corresponding Authors

Wei Zhou – State Key Laboratory of Water Resources and Hydropower Engineering Science, Wuhan University, Wuhan 430072, China; Email: zw mxx@whu.edu.cn

Mathieu Bauchy — Physics of AmoRphous and Inorganic Solids Laboratory (PARISlab), Department of Civil and Environmental Engineering, University of California, Los Angeles, California 90095, United States; orcid.org/0000-0003-4600-0631; Email: bauchy@ucla.edu

Authors

Longwen Tang – State Key Laboratory of Water Resources and Hydropower Engineering Science, Wuhan University, Wuhan 430072, China; Physics of AmoRphous and Inorganic Solids Laboratory (PARISlab), Department of Civil and Environmental Engineering, University of California, Los Angeles, California 90095, United States Gang Ma – State Key Laboratory of Water Resources and Hydropower Engineering Science, Wuhan University, Wuhan 430072, China

Han Liu – Physics of AmoRphous and Inorganic Solids Laboratory (PARISlab), Department of Civil and Environmental Engineering, University of California, Los Angeles, California 90095, United States; orcid.org/ 0000-0002-4899-9998

Complete contact information is available at: https://pubs.acs.org/10.1021/acs.jpcb.0c08794

Author Contributions

The manuscript was written through contributions of all authors. All authors have given approval to the final version of the manuscript.

Funding

This work was supported by the National Key R&D Program of China (Grant No. 2017YFC0404801), the National Science Fund for Distinguished Young Scholars (Grant No. 51825905), and the National Natural Science Foundation of China (Grant No. 51879206). Part of this work was also supported by the National Science Foundation under Grant Nos. 1762292 and 1944510.

Notes

The authors declare no competing financial interest.

■ ACKNOWLEDGMENTS

This work was supported by the National Key R&D Program of China (Grant No. 2017YFC0404801), the National Science Fund for Distinguished Young Scholars (Grant No. 51825905), and the National Natural Science Foundation of China (Grant No. 51879206). Part of this work was also supported by the National Science Foundation under Grant Nos. 1762292 and 1944510. The numerical calculations presented in this paper were conducted on the supercomputing system in the Supercomputing Center of Wuhan University.

REFERENCES

- (1) Chen, M. Mechanical Behavior of Metallic Glasses: Microscopic Understanding of Strength and Ductility. *Annu. Rev. Mater. Res.* **2008**, 38, 445–469.
- (2) Jang, D.; Greer, J. R. Transition from a Strong-yet-Brittle to a Stronger-and-Ductile State by Size Reduction of Metallic Glasses. *Nat. Mater.* **2010**, *9*, 215–219.

- (3) Pauly, S.; Gorantla, S.; Wang, G.; Kühn, U.; Eckert, J. Transformation-Mediated Ductility in CuZr-Based Bulk Metallic Glasses. Nat. Mater. 2010, 9, 473-477.
- (4) Sun, B. A.; Wang, W. H. The Fracture of Bulk Metallic Glasses. Prog. Mater. Sci. 2015, 74, 211-307.
- (5) Tian, L.; Cheng, Y.-Q.; Shan, Z.-W.; Li, J.; Wang, C.-C.; Han, X.-D.; Sun, J.; Ma, E. Approaching the Ideal Elastic Limit of Metallic Glasses. Nat. Commun. 2012, 3, 1-6.
- (6) Launey, M. E.; Hofmann, D. C.; Johnson, W. L.; Ritchie, R. O. Solution to the Problem of the Poor Cyclic Fatigue Resistance of Bulk Metallic Glasses. PNAS 2009, 106, 4955-4956.
- (7) Hess, P. A.; Menzel, B. C.; Dauskardt, R. H. Fatigue Damage in Bulk Metallic Glass II: Experiments. Scr. Mater. 2006, 54, 355-361.
- (8) Menzel, B. C.; Dauskardt, R. H. Stress-Life Fatigue Behavior of a Zr-Based Bulk Metallic Glass. Acta Mater. 2006, 54, 935-943.
- (9) Davis, L. A. Fatigue of Metallic Glasses. J. Mater. Sci. 1976, 11,
- (10) Jia, H.; Wang, G.; Chen, S.; Gao, Y.; Li, W.; Liaw, P. K. Fatigue and Fracture Behavior of Bulk Metallic Glasses and Their Composites. Prog. Mater. Sci. 2018, 98, 168-248.
- (11) Verduzco, J. A.; Hand, R. J.; Davies, H. A. Fatigue Behaviour of Fe-Cr-Si-B Metallic Glass Wires. Int. J. Fatigue 2002, 24, 1089-1094.
- (12) Hess, P. A.; Dauskardt, R. H. Mechanisms of Elevated Temperature Fatigue Crack Growth in Zr-Ti-Cu-Ni-Be Bulk Metallic Glass. Acta Mater. 2004, 52, 3525-3533.
- (13) Wang, G. Y.; Qiao, D. C.; Yokoyama, Y.; Freels, M.; Inoue, A.; Liaw, P. K. Effects of Loading Modes on the Fatigue Behavior of Zr-Based Bulk-Metallic Glasses. J. Alloys Compd. 2009, 483, 143-145.
- (14) Launey, M. E.; Busch, R.; Kruzic, J. J. Effects of Free Volume Changes and Residual Stresses on the Fatigue and Fracture Behavior of a Zr-Ti-Ni-Cu-Be Bulk Metallic Glass. Acta Mater. 2008, 56, 500-510.
- (15) Launey, M. E.; Busch, R.; Kruzic, J. J. Influence of Structural Relaxation on the Fatigue Behavior of a Zr41.25Ti13.75Ni10-Cu12.5Be22.5 Bulk Amorphous Alloy. Scr. Mater. 2005, 54, 483-487.
- (16) Wang, G. Y.; Liaw, P. K.; Morrison, M. L. Progress in Studying the Fatigue Behavior of Zr-Based Bulk-Metallic Glasses and Their Composites. Intermetallics 2009, 17, 579-590.
- (17) Sha, Z. D.; Qu, S. X.; Liu, Z. S.; Wang, T. J.; Gao, H. Cyclic Deformation in Metallic Glasses. Nano Lett. 2015, 15, 7010-7015.
- (18) Maloney, C. E.; Lemaître, A. Amorphous Systems in Athermal, Quasistatic Shear. Phys. Rev. E 2006, 74, No. 016118.
- (19) Şopu, D.; Stukowski, A.; Stoica, M.; Scudino, S. Atomic-Level Processes of Shear Band Nucleation in Metallic Glasses. Phys. Rev. Lett. 2017, 119, 195503.
- (20) Falk, M. L.; Langer, J. S. Dynamics of Viscoplastic Deformation in Amorphous Solids. Phys. Rev. E 1998, 57, 7192-7205.
- (21) Falk, M. L.; Langer, J. S. Deformation and Failure of Amorphous, Solidlike Materials. Ann. Rev. of Conden. Mat. Phys. 2011, 2, 353-373.
- (22) Wang, X. D.; Qu, R. T.; Liu, Z. Q.; Zhang, Z. F. Evolution of Shear-Band Cracking in Metallic Glass under Cyclic Compression. Mater. Sci. Eng., A 2017, 696, 267-272.
- (23) Nosé, S. A Unified Formulation of the Constant Temperature Molecular Dynamics Methods. J. Chem. Phys. 1984, 81, 511-519.
- (24) Hoover, W. G. Canonical Dynamics: Equilibrium Phase-Space Distributions. Phys. Rev. A 1985, 31, 1695-1697.
- (25) Mendelev, M. I.; Kramer, M. J.; Ott, R. T.; Sordelet, D. J.; Yagodin, D.; Popel, P. Development of Suitable Interatomic Potentials for Simulation of Liquid and Amorphous Cu-Zr Alloys. Philos. Mag. 2009, 89, 967-987.
- (26) Plimpton, S. Fast Parallel Algorithms for Short-Range Molecular Dynamics. J. Comput. Phys. 1995, 117, 1–19.
- (27) Barkema, G. T.; Mousseau, N. Event-Based Relaxation of Continuous Disordered Systems. Phys. Rev. Lett. 1996, 77, 4358-4361.
- (28) Cancès, E.; Legoll, F.; Marinica, M.-C.; Minoukadeh, K.; Willaime, F. Some Improvements of the Activation-Relaxation

- Technique Method for Finding Transition Pathways on Potential Energy Surfaces. J. Chem. Phys. 2009, 130, 114711.
- (29) Fan, Y.; Iwashita, T.; Egami, T. How Thermally Activated Deformation Starts in Metallic Glass. Nat. Commun. 2014, 5, 5083.
- (30) Fan, Y.; Iwashita, T.; Egami, T. Energy Landscape-Driven Non-Equilibrium Evolution of Inherent Structure in Disordered Material. Nat. Commun. 2017, 8, 15417.
- (31) Kallel, H.; Mousseau, N.; Schiettekatte, F. Evolution of the Potential-Energy Surface of Amorphous Silicon. Phys. Rev. Lett. 2010, 105, No. 045503.
- (32) Xu, B.; Falk, M. L.; Li, J. F.; Kong, L. T. Predicting Shear Transformation Events in Metallic Glasses. Phys. Rev. Lett. 2018, 120,
- (33) Prieziev, N. V. Shear Band Formation in Amorphous Materials under Oscillatory Shear Deformation. Metals 2020, 10, 300.
- (34) Charbonneau, P.; Kurchan, J.; Parisi, G.; Urbani, P.; Zamponi, F. Fractal Free Energy Landscapes in Structural Glasses. Nat. Commun. 2014, 5, 1-6.
- (35) Hwang, H. J.; Riggleman, R. A.; Crocker, J. C. Understanding Soft Glassy Materials Using an Energy Landscape Approach. Nat. Mater. 2016, 15, 1031-1036.
- (36) Berthier, L.; Biroli, G. Theoretical Perspective on the Glass Transition and Amorphous Materials. Rev. Mod. Phys. 2011, 83, 587-
- (37) Gagnon, G.; Patton, J.; Lacks, D. J. Energy Landscape View of Fracture and Avalanches in Disordered Materials. Phys. Rev. E 2001, 64, No. 051508.
- (38) Xu, B.; Falk, M.; Li, J.; Kong, L. Strain-Dependent Activation Energy of Shear Transformation in Metallic Glasses. Phys. Rev. B 2017, 95, 144201.